OPTICA

# Fast shaping control of x ray beams using a closed-loop adaptive bimorph deformable mirror

SIMON G. ALCOCK,[1,*] IOANA-THEODORA NISTEA,[1] VIVEK G. BADAMI,[2] RICCARDO SIGNORATO,[3] MATTEO FUSCO,[4] LINGFEI HU,[1] HONGCHANG WANG,[1] AND KAWAL SAWHNEY[1]

[1]Diamond Light Source Ltd, Harwell Science & Innovation Campus, Didcot, Oxfordshire, OX11 0DE, UK
[2]Zygo Corporation, Middlefield, Connecticut 06455, USA
[3]S.RI. Tech, Vigonza, Italy
[4]CAEN, Viareggio, Italy
*Corresponding author: simon.alcock@diamond.ac.uk

Received 22 September 2022; revised 18 November 2022; accepted 8 December 2022; published 25 January 2023

**High-speed adaptive correction of optics, based on real-time metrology feedback, has benefitted numerous scientific communities for several decades. However, it remains a major technological challenge to extend this concept into the hard x ray regime due to the necessity for active mirrors with single-digit nanometer height errors relative to a range of aspheric forms. We have developed a high-resolution, real-time, closed-loop "adaptive" optical system for synchrotron and x ray free electron laser (XFEL) applications. After calibration of the wavefront using x ray speckle scanning, the wavefront diagnostic was removed from the x ray beam path. Non-invasive control of the size and shape of the reflected x ray beam was then demonstrated by driving a piezoelectric deformable bimorph mirror at ∼1 Hz. Continuous feedback was provided by a 20 kHz direct measurement of the optical surface with picometer sensitivity using an array of interferometric sensors. This enabled a non-specialist operator to reproduce a series of pre-defined x ray wavefronts, including focused or non-Gaussian profiles, such as flattop intensity or multiple split peaks with controllable separation and relative amplitude. Such changes can be applied in any order and in rapid succession without the need for invasive wavefront diagnostic sensors that block the x ray beam for scientific usage. These innovations have the potential to profoundly change how x ray focusing elements are utilized at synchrotron radiation and XFEL sources and provide unprecedented dynamic control of photon beams to aid scientific discoveries in a wide range of disciplines.**



https://doi.org/10.1364/OPTICA.476449

## 1. INTRODUCTION

A series of fixed-curvature or bendable optics is used on each experimental "beamline" at synchrotron light or free electron laser (XFEL) facilities to focus or collimate ultra-intense x ray beams from the source to the sample under test [1]. Due to the typical grazing angle of incidence of a few milliradians needed for efficient total external reflection of x ray photons, coupled with typical beam widths of a few millimeters, x ray mirrors are typically cuboids with lengths spanning from 25 to 1500 mm, and widths and depths between 20 and 100 mm. The optical face of the single-crystal silicon or fused silica substrate is pre-polished to a range of profiles, including cylinders or ellipses, and is often coated with metallic layers to enhance x ray reflectivity. The optical layout of each synchrotron or XFEL beamline is bespoke to suit a range of experimental techniques, including combinations of x ray diffraction, spectroscopy, ptychography, and imaging. Each beamline can be reconfigured to vary multiple experimental parameters, including changes in x ray wavelength, and the size or location of the focal spot.

Bimorph deformable mirrors have been extensively used by many optical communities for several decades [2]. Such optics are often operated in closed-loop at a refresh rate of hundreds or even thousands of cycles per second, based on feedback from a variety of metrology sensors. However, since hard x rays (10 keV = 0.124 nm) have a wavelength ∼5000 times smaller than red light (633 nm), tuning and stabilizing the surface of an x ray bimorph mirror is several orders of magnitude more demanding than for visible light. Typically, the optical surface of an x ray mirror needs to be optimized to the desired profile with single-digit nanometer height errors. Piezoelectric deformable bimorph x ray mirrors were originally developed at the ESRF, France, in the 1990s [3,4], then at Spring-8, Japan [5], before being commercialized by Thales-SESO, France. X-ray bimorphs are now deployed on many beamlines around the world [6–8]. Their achromatic nature provides beam shaping control over a wide range of x ray wavelengths. Over the past decade, there has been an extensive collaborative research project [9] to advance the performance of bimorph mirrors at Diamond Light Source (Diamond), the United Kingdom's national facility for synchrotron radiation science [10].

When compared to mechanically bent mirrors (typically employing one or two independent bending motors [11]), which can only achieve cylindrical or elliptical profiles, the extra degrees of bending freedom and zonal control of bimorph x ray mirrors (typically with between 8 and 32 electrodes) permit more sophisticated control of the optical surface and the reflected x ray wavefront. This includes correcting opto-mechanical clamping of the mirror, photon-induced heat bumps [12], thermal deformation due to ambient temperature changes, residual polishing errors [13,14], and higher-order aberrations in the wavefront caused by other imperfect optics in the same photon delivery system [15]. A recent article [16] provides an extensive historical review of x ray optics, including the state-of-the-art in wavefront preservation techniques to achieve diffraction-limited performance. This topic is becoming increasingly important as many synchrotron and XFEL facilities upgrade their particle accelerators to produce brighter, more coherent x ray beams.

Active x ray optics for synchrotron and XFEL beamlines have always been driven quasi-statically in open-loop mode. Changes to the shape of the mirror's profile are only made every few hours or days. In extreme cases, active mirrors are not adjusted for many months or even years. But with ever brighter x ray sources, coupled with advances in detector technology and data processing, the throughput of samples has increased significantly in recent years. Many beamlines, particularly those dedicated to macro-molecular crystallography, routinely measure hundreds, and sometimes thousands, of samples per day. Such beamlines now desire to rapidly manipulate the size and shape of the x ray beam, without loss of flux, to suit the dimensions of each crystal or to illuminate different sized regions of larger samples. However, there is an intrinsic constraint in rapidly applying major changes to the photon beam: operated in open-loop, the curvature of x ray bimorph mirrors can drift by several percent over many hours after a large voltage change [17]. This leads to corresponding time variation in the size and shape of the reflected x ray beam. There is also a significant time lag between a change requested by the operator and the reaction of the complex system. Such parasitic drifts will become increasingly problematic as facilities create smaller, brighter x ray sources and employ strong focusing geometries. This motivates the development of a fast, non-invasive, closed-loop "adaptive" bimorph system, based on accurate nano-metrology feedback, which can make large and frequent changes to the size of the x ray beam. Importantly, to maximize scientific usage of the x rays, the closed-loop system should not attenuate or block the beam.

## 2. MATERIALS AND METHODS

### A. System Overview

Figure 1 illustrates the main components and basic operational flow of the closed-loop x ray optical system: a piezoelectric bimorph deformable x ray mirror, a programmable HV-ADAPTOS high-voltage (HV) bipolar power supply, a multi-sensor ZPS interferometer system mounted on an independently supported metrology frame via three bipod flexures, a ZPS controller unit, and a PC.

### B. Bimorph Piezo Deformable X Ray Mirror

The bimorph mirror is an early second-generation optical system, manufactured in 2013 by Thales-SESO, France [18,19]. The 640 mm long substrate has 16 piezo electrodes. Unlike mechanically bent mirrors, bimorph mirrors can work continuously in ultra-high vacuum conditions without heating issues since the piezo actuators draw only a few μA of current for short periods. This feature, coupled with zonal control, makes them ideal candidates for continuous, real-time, high-spatial resolution, adaptive correction of photon beams. The mirror's holder was custom designed by S.RI.Tech, Italy, to reduce the amount of mechanical strain imparted to the mirror [20] and was manufactured by Strumenti Scientifici Cinel, Italy. Multiple studies have shown that the long-term response of bimorph mirrors is linear: height changes induced in the optical surface by applying voltage to individual piezo actuators can be added to accurately predict the global outcome of applying all such voltage changes concurrently. Assuming stable beamline conditions, a bimorph will asymptotically approach a repeatable, quasi-static state over several hours when a given set of piezo voltages is applied. Many beamlines employ lookup tables when they infrequently bend the mirror to switch between focal positions. However, when large and frequent changes are applied, the mirror operates in a dynamic, non-equilibrium state. In this instance, the optimum voltages required to bend the mirror to a given shape will depend on the recent bending history of the substrate, as will be demonstrated in Section 3.A.

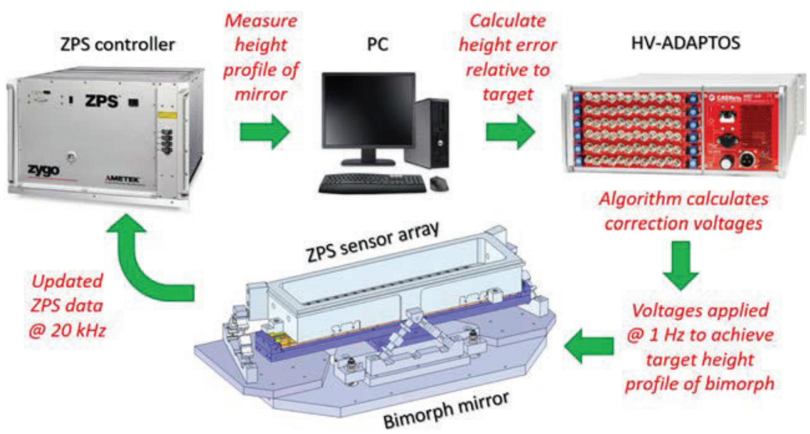


**Fig. 1.** Schematic diagram showing the main hardware components and procedures for autonomous closed-loop control of the bimorph x ray mirror at 1 Hz based on interferometric feedback.

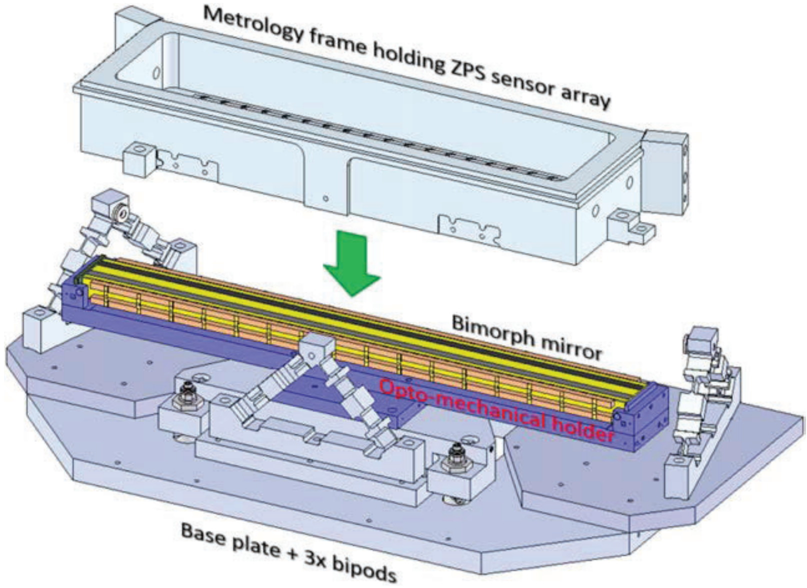


**Fig. 2.** Exploded view of the metrology frame and bimorph system. Bimorph mirror (yellow) is mounted into a holder (blue), which is attached to the base plate (dark gray) containing three bipod flexures. The metrology frame (light gray), holding an array of ZPS interferometric sensors, is mated with the three bipods. This arrangement securely holds the ZPS sensors ∼3.5 mm above the optical surface of the bimorph mirror whilst allowing line-of-sight access for grazing angle of incidence x rays. The bipod flexures ensure that the metrology frame is largely insensitive to thermal changes and is decoupled from the bimorph mirror, thereby providing an ultra-stable reference.

### C. ZPS Multi-Sensor Interferometric System and Metrology Frame

Strain gauges or capacitive displacement sensors have previously been used to monitor the low-order bending of active x ray mirrors [21,22]. However, neither technology directly monitors the optical surface but instead infers its shape by monitoring the back face of the mirror, or by comparison with calibration tables derived from visible light metrology tests conducted prior to beamline installation. Previous work by our group [23] extended this idea to resolve higher-order spatial changes by direct and simultaneous measurement of the bimorph mirror's optical surface at multiple locations using an array of ZPS interferometric position sensors [24] from Zygo Corp., USA [25]. For this work, the height profile of the bimorph mirror was measured using an array of two rows of 19 ZPS sensors. Height changes observed by the ZPS interferometers were in agreement within a few tens of picometers per volt applied to the piezo actuators [26] in comparison with the Diamond-NOM slope profiler and a Zygo Verifire HDX Fizeau interferometer in the Optics Metrology Lab (OML) at Diamond [27]. The fast acquisition rate (up to 208 kHz) of the ZPS, with sub-nanometer sensitivity, makes it an ideal metrology instrument to record dynamic changes in active optics. In contrast to other approaches, where displacement sensors are mounted to the same structure that applies bending force to the mirror, ZPS sensors were kinematically constrained in a separate, decoupled metrology frame, as shown in Fig. 2. This aluminum frame was mounted in a kinematically decoupled fashion to the base plate via three bipod flexures. Finite element modeling showed that the sag of the metrology frame was only ∼0.65 nm for a temperature change of 0.1 K, thereby providing a highly stable, quasi-temperature-invariant support platform for the ZPS sensors. Further details about the mounting hardware and the reasons for material choices are provided in [25].

### D. High-Voltage Power Supply

The HV-ADAPTOS [28] is a programmable bipolar power supply manufactured by CAEN, Italy, and distributed by S.RI. Tech, Italy. This model provides stabilized HVs to most bimorph mirrors at Diamond and at many other synchrotrons and XFEL facilities around the world. In standard operation, voltages are applied slowly (∼10 V/s) in open-loop, either via a Web-based user interface or through shell scripts in the EPICS control system [29] used on all beamlines at Diamond. For a previous project [30], the control software was upgraded to enable open-loop compensation of piezoelectric creep for a list of predetermined voltage shifts. For this current work, major modifications were made to the HV-ADAPTOS software by S.RI. Tech to enable closed-loop operation at ∼1 Hz based on ZPS input data. The refresh rate is currently limited by the software implementation on-board the HV-ADAPTOS. However, the electronics of the ZPS sensors and the HV-ADAPTOS can both operate significantly faster. Hence, with software modifications, there is scope to increase the refresh rate to ∼100 Hz. This enhancement could be used to quasi-continuously drive the mirror through a series of height profiles or to compensate for low frequency vibrations. However, a faster refresh rate may excite mechanical resonances of the system. Further work is required to study bending and rigid body modes of oscillation excited by rapid changes in voltages.

### E. Closed-Loop Architecture

Multi-channel interferometer data is streamed at 20 kHz from the ZPS controller unit to a dedicated PC over a Serial Rapid Input Output (sRIO) high-speed protocol connection. Processed data are transmitted from the PC to the HV-ADAPTOS via a local network Ethernet TCP connection. HV-ADAPTOS CPU receives and processes the latest height data from the ZPS sensors and then computes the difference between the target shape of the mirror and its current shape. Finally, correction voltages are autonomously calculated through a proprietary algorithm and applied to the electrodes of the bimorph mirror's piezo actuators. Target height profiles, stored on-board the HV-ADAPTOS, can be manually toggled via the GUI or scripted to change at specific times, thereby enabling two basic modes of closed-loop operation. The simplest mode is to indefinitely "freeze" the mirror in its current shape: once the user has optimized the size and/or shape of the x ray beam, they initiate closed-loop control and lock the bimorph mirror to its current shape, thereby preserving the focal quality of the x ray beam. The second mode of operation bends the mirror into a series of pre-defined height profiles, each with a user-defined dwell time. For the first time, this dynamic capability enables a non-specialist beamline user to rapidly switch and stabilize between different x ray beam profiles as a function of time. For both modes, the control algorithm monitors for dynamic drifts in the shape of the mirror and quickly nullifies them to lock the optical surface into the required profile(s) with sub-nanometer sensitivity. Further technical details are provided in Supplement 1.

### F. X-Ray Tests

X-ray experiments were conducted at the Test Beamline (B16) at Diamond [31]. A double multilayer monochromator (DMM) selected an unfocused monochromatic beam of x rays with an energy of 15.5 keV from the "broadband" bending magnet source and directed the beam at a grazing incidence of 3 mrad onto the bimorph mirror's surface. The bimorph mirror and the metrology frame containing the ZPS sensor array were securely mounted in a vertical focusing geometry on a stack of motorized goniometer and translation stages, located 43.555 m downstream of the x ray source. An x ray detector was placed 3.2 m downstream of the mirror at the focal plane. The mirror-to-detector distance was chosen such that, with zero volts applied to all piezo electrodes, the pre-polished, cylindrical curvature of the mirror would nominally focus the x rays to the detector position. A schematic of the beamline setup is shown in Fig. 3.

### G. Optimization of the X Ray Beam Profile

The x ray speckle scanning (XSS) technique [32] directly measures the local curvature of the x ray wavefront. A focused x ray beam has a spherical wavefront, where the local radius of the curvature $R$ is constant and matches the distance between the focus and the detector position. To begin optimization, the XSS method measured the reflected x ray wavefront as voltages were sequentially applied to each piezo. These piezo response functions (PRFs) quantify how changing the shape of the mirror modifies the x ray wavefront. Using the x ray PRFs and the wavefront error, voltages were iteratively computed and applied to bend the mirror to optimally focus the x ray beam at the detector position [33]. This method also corrects wavefront distortions caused by other non-perfect optics, such as the DMM, located upstream of the bimorph mirror.

### H. Indirect and Non-Invasive Control of X Ray Wavefront

Many variants of sensors are used to monitor x ray beams at synchrotron and XFEL sources and guide the alignment and curvature optimization of active mirrors to achieve the desired wavefront [34–36]. Ideally, such a sensor should be non-invasive and not cause appreciable attenuation or distortion to the x ray beam. This enables the transmitted x ray beam to be continuously and efficiently used for scientific investigations. Non-invasive sensors are now available [37], but they lack the required spatial or phase sensitivity to accurately characterize x ray wavefronts. Alternatively, other diagnostic instruments have the required spatial sensitivity but are invasive and/or take many seconds or minutes to record the

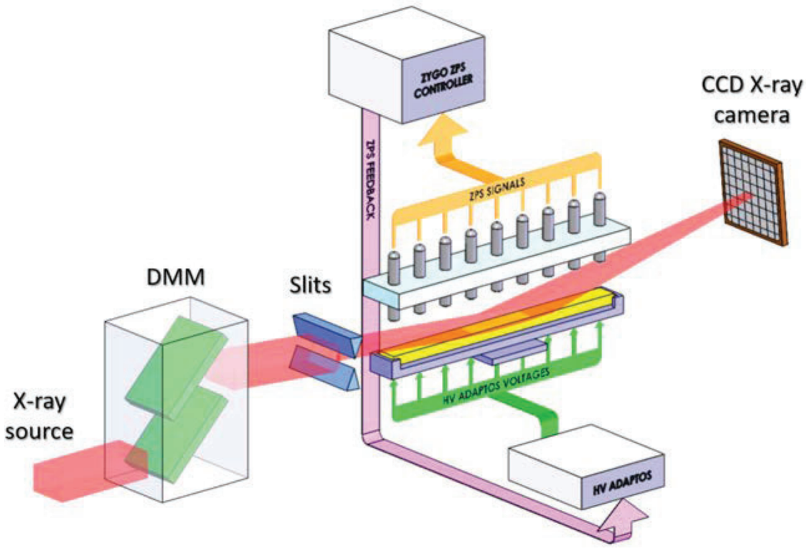


**Fig. 3.** Schematic of the closed-loop bimorph apparatus installed on the B16 Test beamline at Diamond for x ray testing. A double multilayer monochromator (DMM) selected the desired x ray wavelength from the polychromatic bending magnet source. Motorized slits defined the size of the x ray beam illuminating the bimorph mirror. X-rays reflected from the bimorph mirror were imaged using an x ray CCD camera. The array of ZPS interferometers non-invasively measured the optical surface of the bimorph mirror throughout x ray tests and stream data to the HV-ADAPTOS power supply to apply voltage correction to the bimorph mirror's piezo actuators.

wavefront. Currently, a sensor is not commercially available that can concurrently provide real-time, non-invasive measurement of the x ray wavefront with sufficient spatial sensitivity to achieve diffraction-limited performance [16,38].

To mitigate this problem, we propose a two-step process. First, the x ray wavefront is characterized using XSS and corrected to the desired profile using the PRF and inverse-matrix method described in Section 2.H. Second, the ZPS sensors record the shape of the x ray mirror, which produces the required reflected x ray wavefront. This calibration process is repeated for multiple desired x ray wavefronts, including generation of a focused x ray beam and a series of flattop intensity profiles. After removing the x ray wavefront sensor from the beam path, the bimorph can be rapidly driven to any of the pre-recorded target shapes and instantly stabilized with sub-nm accuracy using closed-loop feedback from the ZPS interferometric sensors. Assuming that other components on the beamline are not significantly drifting, this scheme provides fast, indirect, and non-invasive switching and control of the X ray wavefront.

## 3. RESULTS

### A. Curvature Drift of a Bimorph Mirror Operating in Open-Loop Mode

Dynamic drift of the mirror's curvature is influenced by multiple factors, including piezoelectric creep of the actuators, strain or hysteresis from the mirror's opto-mechanical holder that resists piezo bending, and differential thermal expansion between components caused by ambient temperature changes. The latter effect is usually negligible for optics operating in stable conditions under vacuum. At many facilities, the photon-induced heat bump is approximately constant in time, but this assumption cannot be guaranteed in the future for upgraded third- or fourth-generation light sources. A demonstration of parasitic curvature drift is shown in Fig. 4. The change in "sagitta" or sag of the bimorph mirror (depth at the center, relative to its two ends) operating in open-loop was measured by the ZPS interferometers while large voltage jumps were commanded to occur at hourly intervals to create major changes in the curvature of the mirror. Prior to the start of the test, the mirror was allowed to stabilize for many hours with 0 V applied to all electrodes. After 1 hour, a significant 1000 V differential was applied to all piezo actuators to cylindrically bend the mirror. At time $T = 2$ h, all piezos were changed back to 0 V. At $T = 3$ h, all piezos

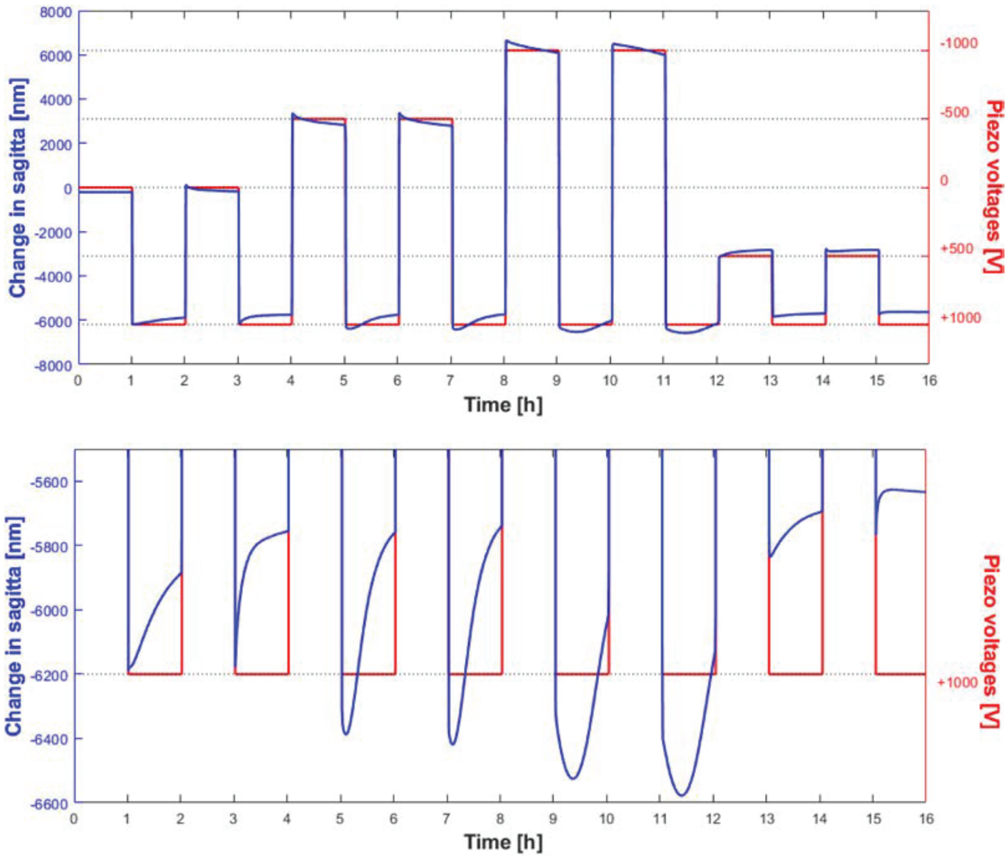


**Fig. 4.** Demonstration of variable sag changes caused by making major changes to the curvature of a bimorph x ray mirror operating in open-loop. The upper chart shows the change in the sagitta of the mirror (blue curve and left-hand vertical axis), as measured by the ZPS interferometer system, as piezo voltages (red curve and right vertical axis) were cycled at hourly intervals. Starting from a very stable state of 0 V, at each odd numbered hour, the mirror's piezo voltages were returned to +1000 V from a range of different starting voltages. Ideally, after each large voltage transition, the mirror's sagitta should exhibit a sharp, square-wave step. However, in the lower chart, showing a zoomed region of the upper chart, the mirror's sagitta variably drifts by hundreds of nanometers on each return to the +1000 V state. Curvature drift degrades the focusing performance of the mirror and limit its usability for fast and accurate operation with x rays.

were driven back to 1000 V. This process of driving the voltages away from the 1000 V set point, and then returning an hour later, was repeated for a range of different voltage jump sizes ($\Delta V = 500$, 1000, 1500, 2000 V), as displayed on the right-hand vertical axis of Fig. 4. Ideally, the sagitta (blue curve and left-hand vertical axis) should display a series of sharply defined, repeatable square-wave functions when voltages are applied to the piezo electrodes (red curve and right-hand vertical axis). However, this is clearly not the case, as is evident in the lower image in Fig. 4, which shows a vertically zoomed plot of the mirror's sagitta for several returns to 1000 V. After the first step change in curvature, subsequent steps have increasingly large drifts of up to 700 nm in the mirror's sagitta that take many hours to settle. This is especially apparent for the most extreme voltage change of 2000 V (corresponding to the full stroke of the mirror and a sagitta change of $>12{,}500$ nm), where the drift of 700 nm corresponds to a 5% error. This is significantly larger than the typical procurement tolerance of $<1\%$ error in the pre-polished radius of synchrotron x ray mirrors. The magnitude and direction of drift are strongly influenced by previous voltage settings applied over the past few hours.

## B. X-Ray Beam Drift Caused by a Bimorph Mirror Operating in Open-Loop Mode

To determine if the magnitude and time scale of curvature drift of the bimorph mirror's optical surface have a measurable effect on the size of the focal x ray beam, the temporal properties of the vertical profile of the x ray beam were continuously measured by the x ray CCD camera while the mirror was repeatedly defocused and then refocused. The bimorph mirror was driven in open-loop mode to the optimized focusing voltages from two very different starting points: first, starting with all piezos at 0 V (i.e., already close to achieving focus) and a second time immediately after a large +1000 V shift had been applied to all piezos to purposefully induce curvature drift in the mirror. The left image in Fig. 5 shows that, when only small voltage changes (10s of volts) were applied to the mirror, the x ray beam was almost instantly focused and remained stable afterward. Conversely, after applying a large voltage excursion of 1000 V before refocusing, the right image in Fig. 5 shows that the width and amplitude of the reflected x ray beam were not well optimized upon refocusing. The x ray beam gradually improved in quality, but even after 5 min it was not fully refocused. To quantify dynamic changes in the x ray beam size, Fig. 6 plots the FWHM vertical width of the x ray beam as a function of time after refocusing. A Lorentzian curve was fitted to remove the background photons in each CCD image, and a Gaussian curve was fitted to the x ray peak to obtain the FWHM. Although drift will eventually stabilize and the x ray beam will asymptotically approach the focused profile, we have demonstrated that open-loop operation of the mirror is not suitable for reliably making large and fast changes to the x ray beam, without waiting for extended periods of time for stabilization to occur.

## C. Closed-Loop Stabilization

To demonstrate the superior performance of closed-loop control, a repeated sequence of voltages was applied to the mirror at 20 s intervals to defocus and then refocus the mirror three times. Defocusing was achieved by simultaneously applying a large differential of −1000 V to all piezos with a fast 300 V/s slew rate to significantly change the mirror's curvature. This process was performed first with the bimorph mirror operating in open-loop, and then it was repeated afterward using closed-loop control. Figure 7 shows temporal snapshots of the x ray beam profile 15 s after each focusing operation in open-loop (red curves) or closed-loop (blue curves). As anticipated, significant drifts and sub-optimal focusing were observed for fast, open-loop operation of the x ray bimorph mirror. For several decades, time-related drifts after a large change in curvature have plagued bimorph x ray mirrors and restricted their usage to quasi-static operation. Conversely, closed-loop operation of the mirror repeatedly and instantly regained perfect focus and remained extremely stable afterward, even after intentionally driving the mirror to extreme voltages to defocus the x ray beam. Closed-loop operation thereby enables the full dynamic potential of bimorph mirrors to be utilized and brings a major improvement in the stability and rapidity of the x ray beam focal quality when fast and significant changes are demanded. Prior to beamline installation, metrology tests in the OML confirmed that the bimorph's shape in closed-loop mode did not exhibit any variation over many hours and was consistently stable at an unprecedented level for active x ray optics of <0.3 nm peak-to-valley (PV) relative to the specified target shape.

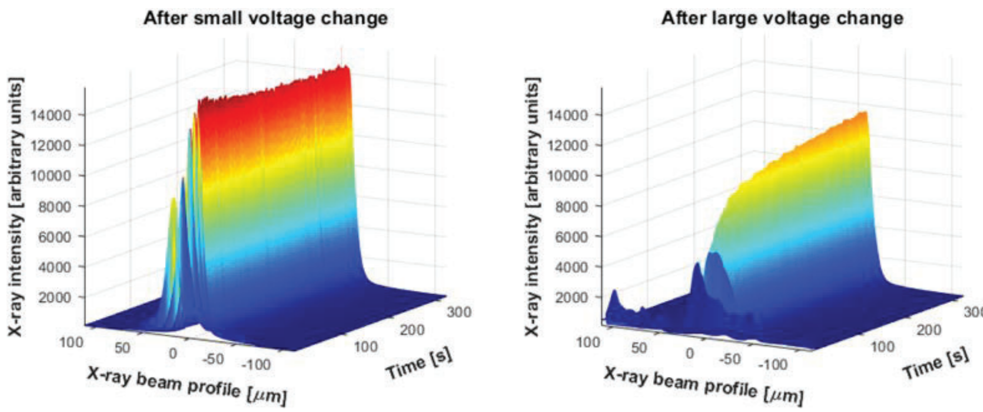


**Fig. 5.** Left image, CCD measurement of the vertical profile of the x ray beam as a function of time over a 5 min period after making small adjustments to the piezo voltages to optimally focus the bimorph mirror. The x ray beam is quickly focused and remains stable thereafter. Right image, repeat of the focusing test, but with a +1000 V differential applied to all piezo actuators immediately before refocusing to purposefully induce a large curvature change in the mirror. In this instance, the x ray beam does not focus rapidly, but slowly drifts toward its asymptotic shape. Even after 5 min, the x ray focus is still not optimized. This demonstrates that the bimorph mirror cannot reliably refocus in open-loop after a large change is made to its curvature.

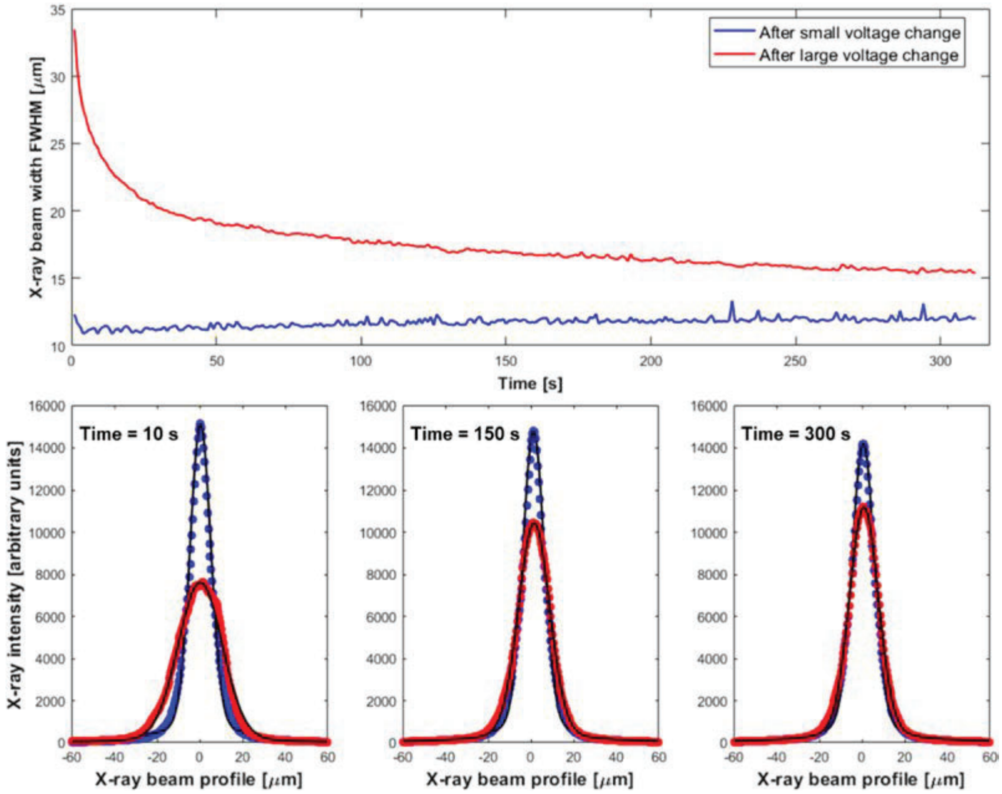


**Fig. 6.** The upper chart displays the dynamic progression of the full width at half-maximum (FWHM) of the vertical profile of the x ray beam during the focusing tests in Fig. 5. After a small voltage change to the bimorph (blue curve), the x ray beam is optimally focused within a few seconds and remains stable thereafter. However, after a large voltage change (red curve), the x ray beam takes many minutes to approach the optimal focus. The lower charts show corresponding temporal snapshots of the measured (black dots) and fitted (lines) cross-sectional profiles of the x ray beam after 10, 150, and 300 s for the different refocusing configurations.

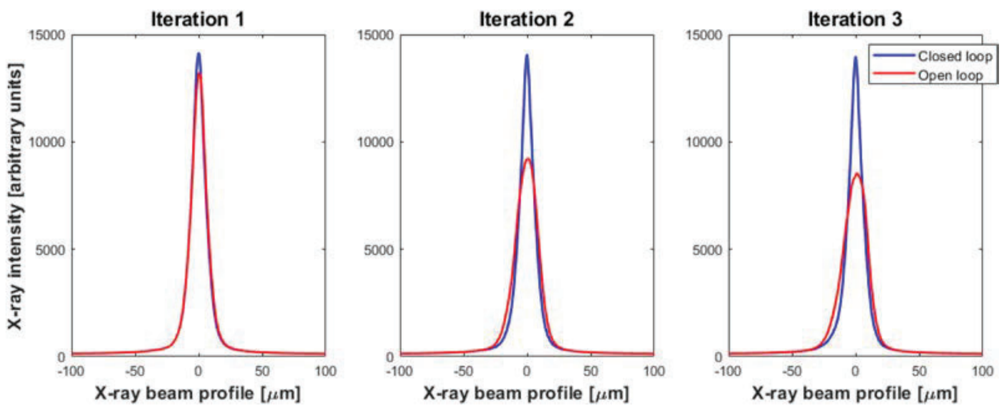


**Fig. 7.** To demonstrate the speed and accuracy of closed-loop control, the bimorph mirror was purposefully defocused and then refocused three times at 20 s intervals. Each image shows a temporal snapshot of the cross-sectional profile of the x ray beam 15 s after each iteration of refocusing. With closed-loop ZPS interferometer feedback of the bimorph mirror, the x ray focal spot was instantly stabilized (blue curves), even after a major change in the mirror's curvature. Conversely, in open-loop (red curves), the mirror's shape did not quickly return to the optimal focus. A video showing the time evolution of the x ray beam vertical profile is provided in Visualization 1.

### D. Creating X Ray Beams with a Flattop, Constant Intensity Profile

Although photon beam shaping using freeform optics is routinely employed by many visible-light communities [39], it is especially challenging and a novelty in the x ray domain. Nevertheless, beam shaping is becoming increasingly important at synchrotron and XFEL facilities [40], including the conversion of Gaussian x ray beams (naturally produced by the source) into a constant intensity "top-hat" super-Gaussian profiles of selectable width. The x ray beam size, typically ranging from $<100$ nm to 150 μm, is chosen to match to the dimension of the sample, or to achieve a specific spatial resolution. Small amounts of deliberate defocusing can create wider reflected x ray beams to probe larger regions of interest on the sample. However, even optical height errors as small as

~5 nm PV can introduce non-negligible intensity striations into out-of-focus x ray beams. An improved method of generating higher-quality, flattop x ray profiles is adding parabolic segments of alternating concave and convex form to the optical surface [41]. The extra degrees of bending freedom offered by a bimorph mirror enable a continuous range of higher-order, re-entrant surface profiles to create x ray beams of user-defined width [42].

The upper image in Fig. 8 shows the vertical profile of the x ray beam as a function of time, as recorded by the CCD camera, while the bimorph mirror was iterated through a sequence of shapes to either focus the x ray beam or create flattop intensity profiles of varying widths. X-ray beam changes were cycled at 10 s intervals in the following sequence: focus (~12 μm FWHM), narrow flattop (~55 μm FWHM), wide flattop (~130 μm FWHM), and back to focus. The lower image in Fig. 8 displays time snapshots of the x ray beam profile during each of the three beam shapes. Intensity striations are present that are correlated to the imperfect polishing quality of this ~10-year-old bimorph mirror (slope error ~500 nrad rms). The "narrow flattop" profile, corresponding to a ~5× magnification of the x ray beam, shows striations that are <10% of the peak intensity. We note that the pattern of striations on the wider flattop x ray beam is very similar, but laterally expanded, compared to the narrow flattop. This provides further evidence that the striations originate from the mirror's intrinsic polishing errors. Previous studies found a strong correlation between the second spatial derivative of optical height errors and the resultant x ray beam striations [43–45]. Furthermore, the congruent shape of the flattop beams confirms that the piezoelectric actuator response is very close to ideal and is not introducing additional distortions to the optical surface. Replacing, or repolishing, the mirror to a current state-of-the-art surface quality (slope error <100 nrad) would significantly reduce the number and amplitude of striations observed in the broadened x ray beam in Fig. 8.

### E. Splitting the X Ray Beam into Multiple, Controllable Peaks

Structured light, rather than uniform or Gaussian illumination, is a field of renewed interest in many scientific disciplines [46]. Bimorph mirrors enable the incident beam to be redistributed into a range of intensity distributions, and even into multiple peaks, without significant loss of photon flux. The vertical intensity distribution of the x ray beam, as measured by the CCD camera, was split into multiple peaks using a simple algorithm to segment the bimorph mirror's optical length into sub-regions. Each sub-region of the mirror was chosen to focus a portion of the x ray beam to a vertically displaced position in the focal plane. By careful choice of the length, angle, and location of each sub-region of the mirror, the user can control the spacing and relative amplitude of the reflected x ray peaks. Starting with a focused x ray beam (black curve), the left image in Fig. 9 shows the x ray beam split into two peaks (blue curve) separated by ~67 μm. This was achieved by applying suitable voltages to the piezo electrodes based on the PRF data to change the amplitude of slope modifications on the bimorph

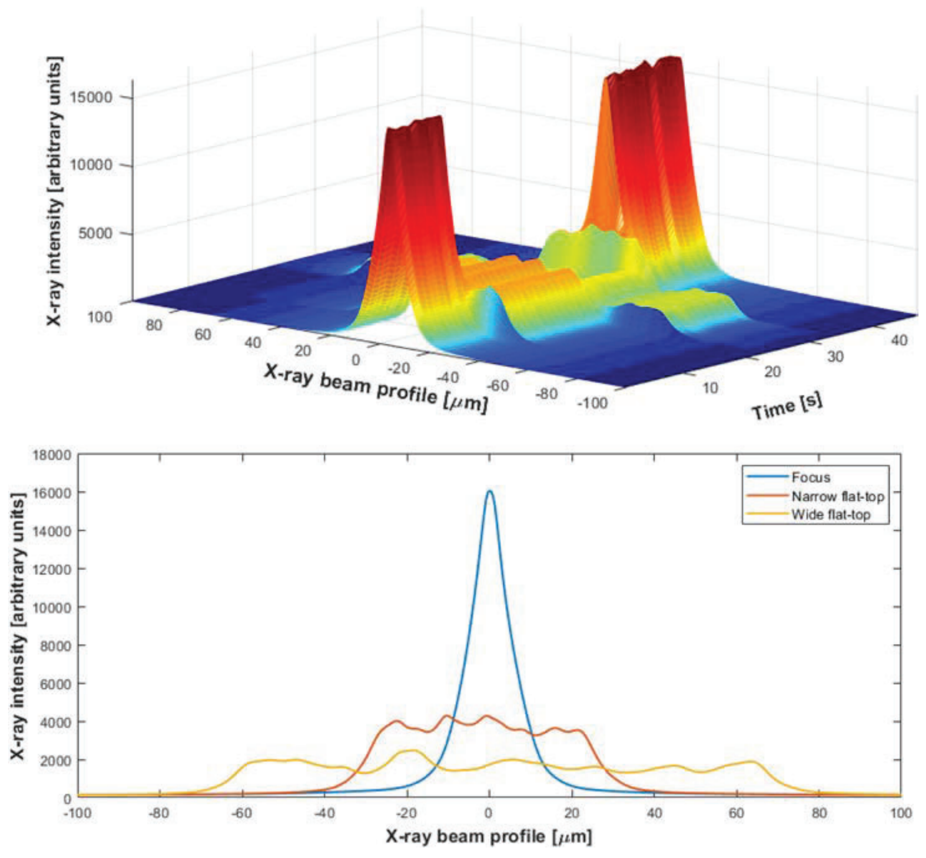


**Fig. 8.** Upper image, vertical profile of the x ray beam as a function of time, as the bimorph mirror was purposefully deformed under closed-loop control to quickly switch between either a focused beam or a constant intensity "flattop" profile of user-defined width. Lower image, super-imposed, time snapshots showing the focused x ray beam and flattop intensity profiles. A video showing the time evolution of the x ray beam is provided in Visualization 2.

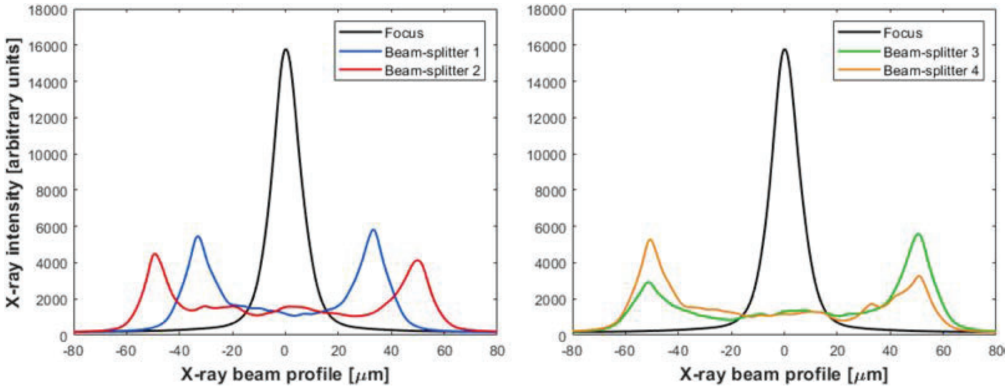


**Fig. 9.** Left image, overlaid x ray beam profiles, as measured by the CCD camera, showing how the focused x ray beam (black curve) can be split into two equal peaks (blue curve), without loss of flux, by applying localized slope changes to the bimorph mirror. The spacing between peaks can also be widened (red curve) by increasing the amplitude of slope changes applied to the mirror. Right image, the relative intensity of each x ray peak can be controlled (green and orange curves). A video showing the time evolution of the x ray beam is provided in Visualization 3.

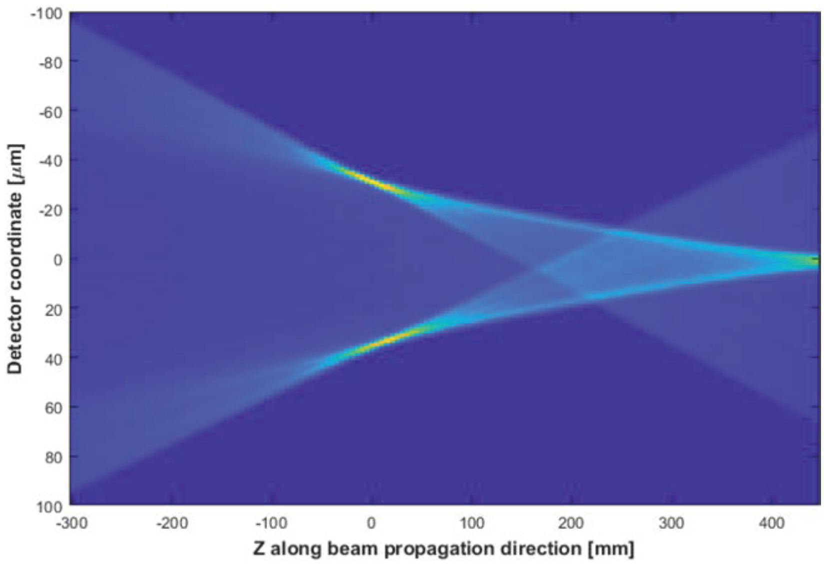


**Fig. 10.** Ray-tracing simulation illustrating how the split x ray peaks propagate along the beamline's optical axis, $Z$. Each vertical slice shows the intensity profile predicted from theory to be recorded by the CCD camera located at each position $Z$ along the length of the beamline. Note that the split peaks are optimized at the focal position where $Z = 0$.

mirror. The spacing between the two x ray peaks was then widened to ~100 µm (red curve) by increasing the amplitude of the slope change. In the right image of Fig. 9, the green and orange curves demonstrate how the relative intensity ratio of each peak in the wider beam splitter can be varied from 50:50 to ~65 : 35. Further details are provided in Supplement 1.

### F. Simulations of the Split X ray Beam Profile

A ray-tracing simulation was performed using the XRT python package [47] to investigate how the split x ray beam propagates through the focal plane. As anticipated, and observed experimentally, Fig. 10 theoretically predicts that the maximum intensity, and corresponding minimum peak width, occurs for both split peaks at the focal position, $Z = 0$. The image was generated by integrating the x ray intensity along the horizontal plane of the detector.

## 4. DISCUSSION AND FUTURE OUTLOOK

Ultimately, the positional stability and cross-sectional profile of the x ray beam is dependent on the dynamic behavior of the x ray source and all optical components on the beamline. The purpose of this work was not to stabilize the x ray beam from all external influences, but to enable fast and repeatable changes in the size and shape of the x ray beam using a closed-loop, adaptive bimorph mirror. Our results demonstrate that other beamline components were sufficiently stable for this scheme to be successful. However, a longer-term goal is to use the full complement of up to 64 ZPS sensors to simultaneously monitor and autonomously correct the angular and linear position of all beamline components, possibly using artificial intelligence schemes. This is an important component of Diamond's strategy to achieve real-time, autonomous control of micro- and nano-focused x ray beams with enhanced quality and versatility, without the intervention of skilled operators. Methodology and hardware could be readily applied to any deformable mirror, regardless of the actuation method. The only change necessary would be to calibrate the response functions of the new mirror to provide accurate inputs for the correction algorithm. Most synchrotrons now operate in "top-up" mode, whereby the circulating electron current is quasi-continuously refilled to account for charge loss. This leads to an almost constant photon-induced heat-load on many beamline optics. However, the increased x ray flux density created by new and upgraded synchrotron light and XFEL sources can create a significant "heat-bump" on the primary optics, which distorts the diffracted or reflected x ray wavefront. A major technical challenge is to find methods to efficiently cool such optics to reduce the magnitude of the distortion. If a cooling manifold were added to the bimorph mirror (for example, adding grooves in the optical substrate to be filled with Ga/In eutectic, and inserting copper cooling blades to conduct heat away without causing vibrations), the closed-loop control system could speculatively be a suitable method to automatically measure and dynamically bend the bimorph mirror to nullify the photon-induced heat bump. This would rapidly correct wavefront distortions caused by time-dependent variations in the incident x ray flux. If bimorph technology is not sufficiently robust to handle the extreme temperature and radiation environment, the ZPS system could provide feedback for a novel scheme [48], which applies time-variable cooling to localized regions of the optic.

## 5. CONCLUSION

We have successfully demonstrated a closed-loop adaptive optical system that can rapidly change and stabilize the shape of x ray beams at synchrotron and XFEL beamlines. For the first time, an x ray bimorph mirror has been rapidly driven and fixed at user-defined target shapes with sub-nanometer sensitivity, based on interferometric feedback operating continuously at 1 Hz. After large changes were made to the x ray beam profile, high-spatial order, time-varying distortions of the optical surface were quickly nullified relative to the ultra-stable reference plane of an array of ZPS distance-measuring sensors embedded in a decoupled metrology frame. Following initial calibration of the x ray wavefront, the invasive x ray sensor was removed from the beam path. Simple, push-button, closed-loop control then enabled a non-specialist operator to quickly alternate between different types of x ray wavefronts without blocking or attenuating the x ray beam, thereby maximizing scientific productivity. Indirect monitoring and control of the x ray wavefront opens a new world of possibilities for applications that require fast and accurate changes in the size and shape of x ray beams. We have shown this can generate non-Gaussian beams, such as flattop intensity profiles or even multiple split peaks with user-controllable separation and relative amplitude. This represents a paradigm shift in using x ray bimorph mirrors at synchrotron light and XFEL sources as real-time "adaptive" optics, operating in a non-equilibrium, dynamic state. *Ex situ* metrology did not observe any long-term damage to the bimorph mirror. One immediate application is serial-crystallography, where many different sized samples are measured in quick succession. Although this technology was developed to aid scientific gains for x ray science, it is hoped that fast, nanoscale control of macroscopic adaptive optics will be of general interest to many other optical communities that require ultra-stability and extreme optical control.

**Funding.** Diamond Light Source Ltd, UK.

**Acknowledgment.** The authors strongly thank Andrew Malandain and Oliver Fox for installing the bimorph mirror at the B16 Test beamline at Diamond Light Source and Andrew Foster for developing EPICS communication protocols with the HV-ADAPTOS. We are also grateful to colleagues in the Optics & Metrology group, especially Hossein Khosroabadi for calculating the x ray power and power density of the beamline, and useful discussions with John Sutter and Andrew Walters. Finally, we acknowledge the work of Andrea Pezzini at CAEN for developing the HV-ADAPTOS hardware.

**Disclosures.** The authors declare no conflicts of interest.

**Data availability.** Data underlying the results presented in this paper are not publicly available at this time but may be obtained from the authors upon reasonable request.

**Supplemental document.** See Supplement 1 for supporting content.

## REFERENCES

1. S. Matsuyama, T. Inoue, J. Yamada, J. Kim, H. Yumoto, Y. Inubushi, T. Osaka, I. Inoue, T. Koyama, K. Tono, H. Ohashi, M. Yabashi, T. Ishikawa, and K. Yamauchi, "Nanofocusing of X-ray free-electron laser using wavefront-corrected multilayer focusing mirrors," Sci. Rep. **8**, 17440 (2018).
2. C. Kettenbeil, J. Jewell, J. K. Wallace, and J. Steeves, "Picometer wavefront sensing using the phase-contrast technique," Optica **7**, 1267–1274 (2020).
3. R. Signorato, "R&D program on multisegmented piezoelectric bimorph mirrors at the ESRF: status report," Proc. SPIE **3447**, 20–31 (1998).
4. R. Signorato, "R&D program on multisegmented piezoelectric bimorph mirrors at the ESRF–status report: II," Proc. SPIE **3773**, 50–59 (1999).
5. R. Signorato and T. Ishikawa, "R&D on third generation multi-segmented piezoelectric bimorph mirror substrates at Spring-8," Nucl. Instrum. Methods Phys. Res. A **467**–468, 271–274 (2001).
6. A. Erko, F. Schäfers, A. Firsov, W. B. Peatman, W. Eberhardt, and R. Signorato, "The BESSY X-ray microfocus beamline project," Spectrochim. Acta B Atom. Spectros. **59**, 1543–1548 (2004).
7. R. Signorato, D. Hausermann, M. Somayazulu, and J.-F. Carré, "Performance of an adaptive u-focusing Kirkpatrick-Baez system for high-pressure studies at the Advanced Photon Source," Proc. SPIE **5193**, 112–123 (2004).
8. S. Matsuyama, H. Nakamori, T. Goto, T. Kimura, K. P. Khakurel, Y. Kohmura, Y. Sano, M. Yabashi, T. Ishikawa, Y. Nishino, and K. Yamauchi, "Nearly diffraction-limited X-ray focusing with variable-numerical-aperture focusing optical system based on four deformable mirrors," Sci. Rep. **6**, 24801 (2016).
9. J. P. Sutter, S. G. Alcock, I. T. Nistea, H. Wang, and K. Sawhney, "Active and adaptive x-ray optics at diamond light source," Synchrotron. Radiat. News **35**(2), 8–13 (2022).
10. "Diamond light source," https://www.diamond.ac.uk.
11. M. Vannoni, I. Freijo Martín, and H. Sinn, "Characterization of an x-ray mirror mechanical bender for the European XFEL," J. Synchrotron. Radiat. **23**, 855–860 (2016).
12. M. Sanchez Del Rio, A. Wojdyla, K. A. Goldberg, G. D. Cutler, D. Cocco, and H. A. Padmore, "Compensation of heat load deformations using adaptive optics for the ALS upgrade: a wave optics study," J. Synchrotron Rad. **27**, 1141–1152 (2020).
13. L. Huang, J. Xue, and M. Idir, "Controlling x-ray deformable mirrors during inspection," J. Synchrotron Rad. **23**, 1348–1356 (2016).
14. M. Vannoni, I. F. Martín, V. Music, and H. Sinn, "Calibration and optimization of an x-ray bendable mirror using displacement-measuring sensors," Opt. Express **24**, 17292–17302 (2016).
15. K. Sawhney, S. Alcock, J. Sutter, S. Berujon, H. Wang, and R. Signorato, "Characterisation of a novel super-polished bimorph mirror," J. Phys. Conf. Ser. **425**, 052026 (2013).
16. D. Cocco, G. Cutler, M. Sanchez del Rio, L. Rebuffi, X. Shi, and K. Yamauchi, "Wavefront preserving x-ray optics for synchrotron and free electron laser photon beam transport systems," Phys. Rep. **974**, 1–40 (2022).
17. S. G. Alcock, J. P. Sutter, K. J. S. Sawhney, D. R. Hall, K. McAuley, and T. Sorensen, "Bimorph mirrors: the good, the bad, and the ugly," Nucl. Instrum. Methods Phys. Res. A **710**, 87–92 (2013).
18. J.-F. Carré, "Bimorph optical element," U.S. patent 8469527 (25 June 2013).

19. S. G. Alcock, I. Nistea, J. P. Sutter, K. Sawhney, J. J. Fermé, C. Thellièr, and L. Peverini, "Characterization of a next-generation piezo bimorph x-ray mirror for synchrotron beamlines," J. Synchrotron Radiat. **22**, 10–15 (2015).
20. S. G. Alcock, I.-T. Nistea, R. Signorato, and K. Sawhney, "Dynamic adaptive x-ray optics. Part I. Time-resolved optical metrology investigation of the bending behaviour of piezoelectric bimorph deformable x-ray mirrors," J. Synchrotron Radiat. **26**, 36–44 (2019).
21. L. A. Poyneer, T. Pardini, T. McCarville, D. Palmer, and A. Brooks, "Control of a 45-cm long x-ray deformable mirror with either external or internal metrology," Proc. SPIE **9208**, 92080F (2014).
22. M. Vannoni, I. F. Martín, S. Smidtchen, T. M. Baumann, M. Meyer, and V. Music, "Metrology characterization of ultraprecise bendable mirrors for the European XFEL: from offsite calibration to installation and commissioning," J. Synchrotron Radiat. **26**, 1110–1114 (2019).
23. S. G. Alcock, I. T. Nistea, V. G. Badami, R. Signorato, and K. Sawhney, "High-speed adaptive optics using bimorph deformable x-ray mirrors," Rev. Sci. Instrum. **90**, 021712 (2019).
24. https://www.zygo.com/products/nano-position-sensors/absolute-position-sensors.
25. V. G. Badami, E. Abruña, L. Huang, and M. Idir, "*In situ* metrology for adaptive x-ray optics with an absolute distance measuring sensor array," Rev. Sci. Instrum. **90**, 021703 (2019).
26. I.-T. Nistea, S. G. Alcock, V. Badami, R. Signorato, and K. J. S. Sawhney, "Controlling an active bimorph deformable mirror with sub-nanometre resolution," Proc. SPIE **11109**, 111090E (2019).
27. I.-T. Nistea, S. G. Alcock, M. Bazan da Silva, and K. J. S. Sawhney, "The optical metrology laboratory at diamond: pushing the limits of nano-metrology," Proc. SPIE **11109**, 1110906 (2019).
28. HV-ADAPTOS, https://www.caenels.com/products/hv-adaptos/.
29. "EPICS 7 Core Status Report," https://www.researchgate.net/publication/336567873_EPICS_7_Core_Status_Report.
30. S. G. Alcock, I. T. Nistea, R. Signorato, R. L. Owen, D. Axford, J. P. Sutter, A. Foster, and K. Sawhney, "Dynamic adaptive x-ray optics. Part II. High-speed piezoelectric bimorph deformable Kirkpatrick–Baez mirrors for rapid variation of the 2D size and shape of x-ray beams," J. Synchrotron Radiat. **26**, 45–51 (2019).
31. K. J. S. Sawhney, I. P. Dolbnya, M. K. Tiwari, L. Alianelli, S. M. Scott, G. M. Preece, U. K. Pedersen, and R. D. Walton, "A test beamline on diamond light source," AIP Conf. Proc. **1234**, 387–390 (2010).
32. H. Wang, J. Sutter, and K. Sawhney, "Advanced in situ metrology for x-ray beam shaping with super precision," Opt. Express **23**, 1605–1614 (2015).
33. H. Wang, K. Sawhney, S. Berujon, J. Sutter, S. G. Alcock, U. Wagner, and C. Rau, "Fast optimization of a bimorph mirror using x-ray grating interferometry," Opt. Lett. **39**, 2518–2521 (2014).
34. M. Idir, D. Cocco, and L. Huang, "Special issue 'EUV and x-ray wavefront sensing'," Sensors **22**, 3940–3943 (2022).
35. H. J. Lee, Y. Feng, G. Marcus, D. Zhu, D. Cocco, M. Seaberg, A. Aquila, J. Krzywinski, B. Nagler, C. Hardin, A. Sakdinawat, F. Seiboth, S. Boutet, Y. Liu, and Y. Ding, "High-accuracy wavefront sensing for x-ray free electron lasers," Optica **5**, 967–975 (2018).
36. M. Seaberg, R. Cojocaru, S. Berujon, *et al.*, "Wavefront sensing at x-ray free-electron lasers," J. Synchrotron Radiat. **26**, 1115–1126 (2019).
37. K. A. Goldberg, A. Wojdyla, and D. Bryant, "Binary amplitude reflection gratings for X-ray shearing and Hartmann wavefront sensors," Sensors **21**, 536 (2021).
38. H. Wang, K. Sawhney, L. Hu, and O. Fox, "Fast wavefront sensing for x-ray optics with an alternating speckle tracking technique," Opt. Express **30**, 33259–33273 (2022).
39. J. P. Rolland, M. A. Davies, T. J. Suleski, C. Evans, A. Bauer, J. C. Lambropoulos, and K. Falaggis, "Freeform optics for imaging," Optica **8**, 161–176 (2021).
40. D. Spiga, L. Raimondi, C. Svetina, and M. Zangrando, "X-ray beam-shaping via deformable mirrors: analytical computation of the required mirror profile," Nucl. Instrum. Methods Phys. Res. A **710**, 125–130 (2013).
41. D. Laundy, K. Sawhney, I. Nistea, S. G. Alcock, I. Pape, J. Sutter, L. Alianelli, and G. Evans, "Development of a multi-lane x-ray mirror providing variable beam sizes," Rev. Sci. Instrum. **87**, 051802 (2016).
42. J. P. Sutter, S. G. Alcock, Y. Kashyap, I. Nistea, H. Wang, and K. Sawhney, "Creating flat-top x-ray beams by applying surface profiles of alternating curvature to deformable piezo bimorph mirrors," J. Synchrotron Radiat. **23**, 1333–1347 (2016).
43. J. P. Sutter, S. G. Alcock, F. Rust, H. Wang, and K. Sawhney, "Structure in defocused beams of x-ray mirrors: causes and possible solutions," Proc. SPIE **9208**, 92080G (2014).
44. L. Hu, H. Wang, J. P. Sutter, and K. Sawhney, "Investigation of the stripe patterns from x-ray reflection optics," Opt. Express **29**, 4270–4286 (2021).
45. D. Cocco and D. Spiga, "Wavefront preserving optics for diffraction-limited storage rings and free-electron lasers," Proc. SPIE **11111**, 37–46 (2019).
46. A. Forbes, M. de Oliveira, and M. R. Dennis, "Structured light," Nat. Photonics **15**, 253–262 (2021).
47. K. Klementiev and R. Chernikov, "Powerful scriptable ray tracing package XRT," Proc. SPIE **9209**, 60–75 (2014).
48. D. Cocco, D. Cocco, C. Hardin, D. Morton, L. Lee, M. L. Ng, L. Zhang, L. Assoufid, W. Grizolli, X. Shi, D. A. Walko, G. Cutler, K. A. Goldberg, A. Wojdyla, M. Idir, L. Huang, and G. Dovillaire, "Adaptive shape control of wavefront-preserving x-ray mirrors with active cooling and heating," Opt. Express **28**, 19242–19254 (2020).